Microscale Simulation of Settler Processes in Copper Matte Smelting

KIM O. FAGERLUND and HEIKKI JALKANEN

The literature survey on previous studies of flash smelting revealed there is very little information published concerning matte- and slag-forming processes in the settling part of the reactor. An experimental study of reaction and separation phenomena, molten phase formation, was carried out by smelting mixtures of oxidation products of chalcopyrite concentrate, silica sand, and slag at typical settler temperatures 1300 °C to 1350 °C. Theoretical aspects and considerations on industrial scale furnaces are discussed, and conclusions are drawn from microscale experiments conducted in this study. A description of the possible reaction and interaction phenomena between molten phases of metal-matte-slag-silica flux is given based on previous knowledge and experiments conducted.

I. INTRODUCTION

SUSPENSION smelting processes, especially the Outokumpu flash smelting process, have become the dominant methods for copper production, accounting for more than 50 pct of the world primary copper capacity. Flash oxidation phenomena taking place in a flash smelting reactor shaft have been quite extensively studied on a laboratory scale[1–8] and to some extent on a pilot and industrial scale.[9–14] In copper smelting, iron sulfide can be regarded as the main impurity. Although iron is selectively oxidized in suspension smelting, it is not removed from the matte unless silica flux is added. Inefficient fluxing and a very high degree of oxidation in the suspension gives rise to the magnetite level in the reaction products. According to the study of Kimura *et al.*,[11] it appears that oxidation reactions are still in progress when the oxidation products impact the slag surface.

There seems to be no common accordance in the literature concerning the extent of slag formation in the suspension. The opinions vary from negligible to remarkable particle collision frequency and progress of slag forming reactions.[11,13–16] The main reason for this might be that the suspension density, particle size and composition, and differences in flight time are different at different smelters.

Matte and slag formation in suspension smelting processes comprise several stages. The first stage involves the primary oxidation of concentrate particles with subsequent melting. Depending on the initial composition of particles, degree of oxidation, and temperature, they are heated to their melting temperature by the reaction heat, and the oxides formed are dissolved in the sulfide phase and precipitated, mainly as magnetite or ferrites. Slag and matte formation proceed largely in the settler, beneath the reaction shaft, when the suspended particles are collected onto the molten slag, and the heterogeneous mixture of reaction products and silica flux meet. The final phase separation stage in the settler includes chemical reactions between the concentrate reaction products and silica, as well as coagulation of droplets followed by settling to the bottom of the reactor by gravitational force.

Only a very limited number of studies have been published concerning matte and slag forming processes in the settling part of the reactor. Genevski *et al.*[17] reported some information on the morphology of the slag surface below the flash smelter reaction shaft. They studied the oxygen and sulfur potentials and the form of slag losses in high-grade matte smelting (72 to 74 pct Cu) at the MDK copper smelter in Bulgaria. The normalized oxygen potential ($\lg p_{O2}$/bar) at 1250 °C, in samples taken below the reaction shaft, and the uptake, vertically as a function of melt depth, was reported to decrease gradually through the slag and matte phases from −5.2 at the slag surface to −7.1 near the bottom of the furnace. This observation contradicts measurements by Kemori and co-workers conducted at the Toyo flash smelting furnace producing medium grade 50 to 58 pct Cu matte.[18] They found the normalized oxygen potential to be nearly constant in the matte, $\lg P_{O2}$/bar ~ −8, and slightly increasing toward the bottom of the settler, $\lg p_{O2}$/bar ~ −7.5, at 1250 °C.

Fundamental knowledge regarding matte and slag formation, the final phase separation, and matte settling in the settler is inadequate. It is virtually impossible to create corresponding conditions in a small scale laboratory furnace. Therefore, the aim of this research was to investigate reaction and separation phenomena, molten phase formation, and matte and slag formation morphology by smelting mixtures of oxidation products of chalcopyrite concentrate, silica sand, and slag at typical settler temperatures of 1300 °C to 1350 °C.

II. THEORETICAL CONSIDERATIONS ON MATTE AND SLAG FORMATION REACTIONS

When the copper concentrate is introduced into the burner, the finest particles heat up and ignite very rapidly, making the fast reactions possible. Basically, chalcopyrite first loses its labile sulfur and transforms into sulfur deficient form, $CuFeS_{2-x}$, often called "intermediate solid solution," Cu_5FeS_4, bornite, and finally, Cu_2S, chalcocite. The smallest particle fraction tends to oxidize thoroughly, whereas the

KIM O. FAGERLUND, Visiting Scientist, is with the G.K. Williams Cooperative Research Centre for Extractive Metallurgy, CSIRO–Division of Minerals, Clayton South, Victoria 3169, Australia. HEIKKI JALKANEN, Professor, is with the Laboratory of Metallurgy, Helsinki University of Technology, 02015 HUT, Finland.

Manuscript submitted March 11, 1999.

biggest particles remain somewhat underoxidized as an average. The observations on the combustion behavior of chalcopyrite have shown that the biggest matte particles will fragment into smaller particles. This is due to explosive discharge caused by the pressure of the molten sulfidic core enclosed by a solid oxide crust.[2,5,19] Matte particles will, therefore, be further oxidized if there is oxygen left in the gas. Kemori *et al.*[13,14] and Kimura *et al.*[11] have reported considerable particle growth along the reaction shaft by collision, indicating slag-forming progression already occuring in the shaft region. Because of the different suspension conditions and grain size distributions, the particle/droplet-gas suspension meeting the slag surface beneath the suspension shaft typically contains reaction products with varying degrees of oxidation, as described by Hagni *et al.*[9,10]

According to the thermodynamic prerequisites of oxidation reactions and experimental evidence from the literature, the probable oxidation course for suspension smelting of chalcopyrite concentrate, consisting mainly of copper-iron and iron sulfides, is described as follows. Iron and sulfur are preferentially oxidized. The part of the iron oxide, that is insoluble in the molten sulfide phase, precipitates in the form of magnetite and ferrites (Figure 1). Superficial oxidation of concentrate particles or molten sulfide droplets is observed to lead to rapid formation of a magnetite crest around the particle, preventing further oxidation if the pressure developed inside the core does not lead to explosive fragmentation. Molten matte is able to dissolve iron oxides, but the solubility decreases with decreasing iron sulfide content, as shown in Figure 2. Therefore, it is obvious that the magnetite formed during the oxidation of iron-sulfide bearing minerals cannot be fully dissolved in the matte where high-grade matte smelting or flash converting is concerned (Figure 1). This fact is fully confirmed by experimental results obtained from laboratory-scale suspension oxidation investigations, as well as the analysis of samples from industrial or pilot scale flash smelting reactors.[11,20,21,22] The oxidation of concentrate particles and droplets in suspension is nonuniform. At the same time as the oxidation degree of a certain fraction of the particles will remain low, another part will exceed the average oxidation level. In high-grade matte smelting, an increasing number of sulfide droplets will reach an oxidation degree at which all the iron sulfide is burned and cuprous sulfide is converted to metallic copper or even to cuprous oxide (copper ferrites).

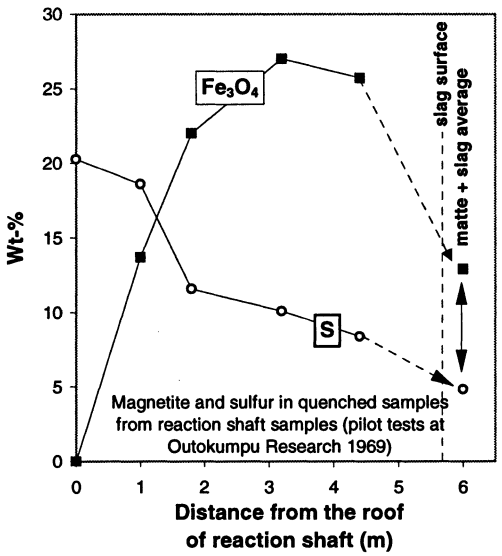

Fig. 1—Magnetite and sulfur content in quenched samples against distance from the roof of the reaction shaft determined in pilot scale flash smelting furnace (data taken from Ref. 20).

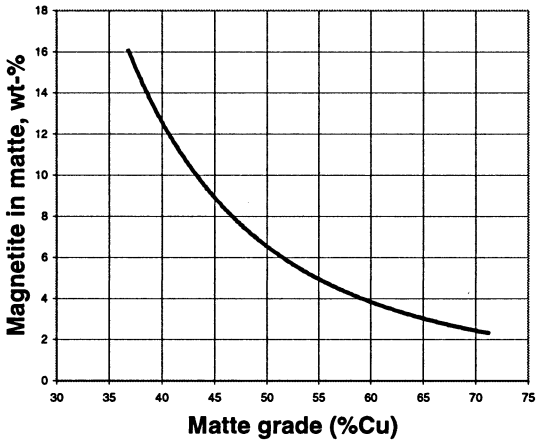

(*a*)

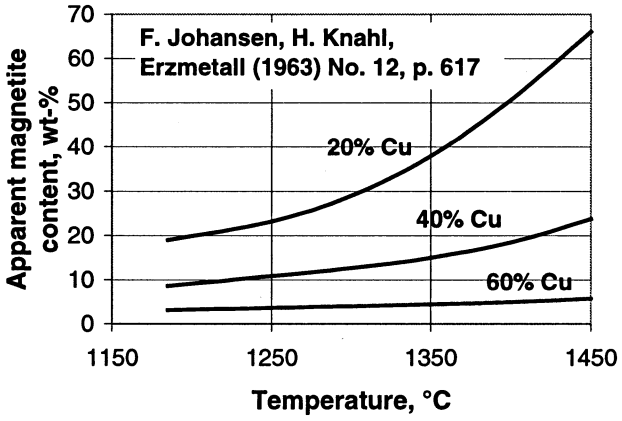

(*b*)

Fig. 2—Solubility of magnetite in copper matte: (*a*) at 1190 °C (data taken from Ref. 21); and (*b*) calculated on the basis of oxygen solubility measurements attributing all oxygen to magnetite (data taken from Ref. 22).

It is quite obvious that desulfurization continues in the settler, where the concentrate oxidation products and nonreacted silica sand collect on the surface of the molten slag layer. As it appears in the study of Kimura *et al.*,[11] and can also be noticed in the results obtained in early studies of the pilot scale flash smelting furnace conducted by Outokumpu Research[20] (Figure 1), the final desulfurization and magnetite reduction reactions must take place in the settler region of the furnace.

Possible reactions for magnetite reduction in the presence of silica and silica bearing slags are

$$3Fe_3O_4\,(s) + \{FeS\}_{matte} + 5SiO_2\,(s) = 5(Fe_2SiO_4)_{slag} + SO_2\,(g) \quad [1]$$

and/or

$$3Fe_3O_4\,(s) + \{FeS\}_{matte} = 10(FeO)_{slag} + SO_2\,(g) \quad [2]$$

and/or

$$2Fe_3O_4\ (s) + \{Cu_2S\}_{matte} + 3SiO_2\ (s) = 3(Fe_2SiO_4)_{slag} + 2Cu\ (l) + SO_2\ (g) \quad [3]$$

Thermodynamic considerations suggest a low probability for Reaction [3], even at unit activity of cuprous sulfide, and the reaction only tends to proceed with very low iron silicate activity and/or sulfur dioxide pressure, *i.e.*, conditions not prevailing in copper matte smelting furnaces. As long as the matte contains some ferrous sulfide, and in addition to direct dissolution of magnetite in slag, Reaction [1] can be considered to be responsible for the elimination of solid magnetite and desulfurization in the settler region of matte smelting furnaces. However, if the sulfur activity in the matte is high, the reaction

$$2Fe_3O_4\ (s) + \{S\}_{matte} + 3SiO_2\ (s) = 3(Fe_2SiO_4)_{slag} + SO_2\ (g) \quad [4]$$

can also play an important role in magnetite reduction. Figure 3 shows the equilibrium relationship between ferrous sulfide or sulfur in the matte phase, and iron orthosilicate in slag, at a sulfur dioxide pressure of 1 atmosphere. This is of special importance as it corresponds to the spontaneous formation of sulfur dioxide gas inside the slag phase. As the activity of iron orthosilicate in the smelter slag can be less than unity, and sulfur activity in matte droplets collecting from the gas to the slag relatively high, especially if the magnetite crust prevents the decomposition of sulfides (pyrite, chalcopyrite, and bornite), both Reactions [1] and [4] may be effective in magnetite reduction.

With the participation of cuprous oxide dissolved in the slag, the possible interaction reactions between matte and slag may be

$$\{FeS\}_{matte} + (Cu_2O)_{slag} + 0.5SiO_2\ (s) = \{Cu_2S\}_{matte} + 0.5(Fe_2SiO_4)_{slag} \quad [5]$$

$$\{FeS\}_{matte} + 3(Cu_2O)_{slag} + 0.5SiO_2\ (s) = 6Cu\ (l) + 0.5(Fe_2SiO_4)_{slag} + SO_2\ (g) \quad [6]$$

$$\{Cu_2S\}_{matte} + 2(Cu_2O)_{slag} = 6Cu\ (l) + SO_2\ (g) \quad [7]$$

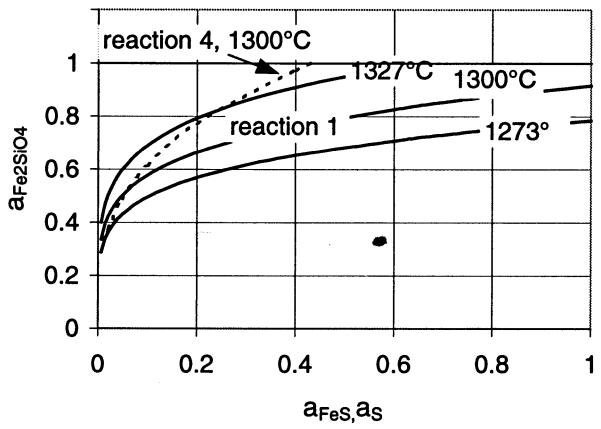

Fig. 3—Equilibrium conditions for magnetite reduction by ferrous sulfide/sulfur in the sulfide phase (matte); sulfur activity related to pure sulfur gas (S_2) at atmospheric pressure; reactions tend to proceed under the conditions prevailing beneath the curves.

Figure 4 shows the equilibrium conditions for Reactions [5] through [7] at constant sulfur dioxide pressure, 1 atmosphere, corresponding to spontaneous desulfurization inside the slag. Reactions tend to proceed above the curves in Figure 4 and, as can be seen, exchange Reaction [5] is favored in this case.

III. EXPERIMENTAL

A. *Apparatus*

The experimental apparatus used in this study comprised: a furnace provided with rod-shaped lanthanum-cromite heating elements, an X-ray imaging system, a video camera, a digital image processing system working with an IBM 486 PC, and the usual PID temperature controlled tube furnaces heated by a silicon carbide element with alumina or mullite as the tube material.

The following observation methods were employed. The water quenched samples or samples obtained by dipping a copper rod onto the slag surface were observed in polished specimens using a light optical microscope (LOM) and scanning electron microscope (SEM) with an energy dispersive spectrometer (EDS) and by chemical methods. Reaction phenomena between molten matte and slag was followed *in situ* using the X-ray transmission technique.

B. *Materials and Preparation*

Oxidized chalcopyrite (OCHP) samples were prepared by treating concentrate in an alumina boat at temperatures of 700 °C, 900 °C, and 1000 °C for 10 to 40 minutes in air atmosphere. The highest oxidation-desulfurization rate was observed at 900 °C, while at 1000 °C, the formation of an oxidation crust markedly decreased the reaction rate. It turned out to be extremely difficult to prepare chalcopyrite concentrate with a highly controlled degree of oxidation simply by oxidation in air. Therefore, highly oxidized chalcopyrite (HOC) was simulated with a synthetic sample prepared by mixing 41 pct CHP concentrate, 28 pct Cu_2O, and 31 pct Fe_3O_4 (calculated to produce ~70 pct Cu matte when smelted), charged in an alumina crucible covered by graphite shamotte crucibles and a lid at 900 °C, for 1/2 hour. In

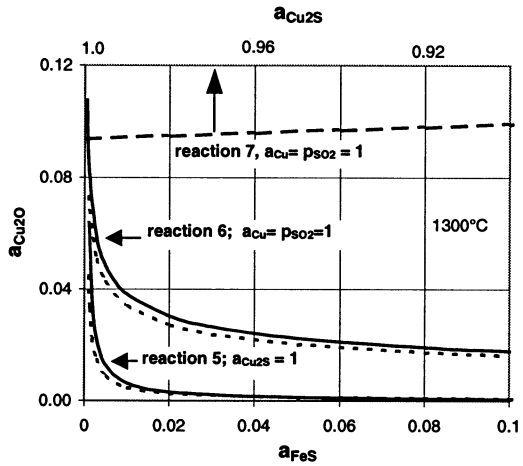

Fig. 4—Equilibrium conditions for ferrous and cuprous sulfide interaction with cuprous oxide at unit activity of silica and sulfur dioxide pressure of one atmosphere; reactions tend to proceed under the conditions prevailing above the curves.

addition to these concentrate materials with varying degrees of oxidation, 62 pct industrial Cu matte (MGIM) and magnetite saturated cuprous sulfide (SHM) were used for reaction, separation, and settling experiments. All the matte analyses are shown in Table I.

The fayalite and wollastonite types of slag were prepared by mixing together Merck Pa grade powders of Fe, Fe_2O_3, SiO_2, and CaO and heating the mixture in alumina crucibles covered by graphite shamotte crucibles and a graphite lid for 1.5 hours at 1350 °C. Oxidized slags were prepared by mixing iron silicate slag with Cu_2O powder and mechanically pressing together using a binding agent. The briquettes were sintered for 2 hours at 900 °C in an Ar atmosphere, slowly cooled, and ground. The wollastonite slag was prepared by adding 22 pct of CaO to the primary fayalite slag. Riedel-de Haën pure silica and industrial sand provided by Outokumpu Harjavalta were used for morphological studies. Industrial sand was studied under the EDS, and the amount of minor elements was found to be insignificant. The average chemical analyses of the slags are shown in Table I.

Alumina crucibles of various size were of Degussit Al 23. Gaseous materials, nitrogen, argon, and air were of commercial grade.

C. *Experimental Procedures*

In this work, three methods were used to simulate the reactions between the oxidation products of chalcopyrite concentrate and molten slag, as well as the coagulation and settling of matte droplets in slag. A large number of polished samples and video images from X-ray visualization were investigated using the following methods.[23,24,25]

(1) Reaction smelting of solid mixtures in a crucible placed in a fused quartz ampoule (simplified schematic presentation in Figure 5). In most cases, the alumina crucible had a diameter of 3 cm and a height of 4 cm, but a smaller size (o.d. 2 and height-3 cm) was also used. The length of the quartz ampoule (50 to 60 cm) was chosen according to the furnace used so that the upper side would remain outside the heated area, and the inert gas (Ar or N_2) could be passed through the capillary tube to prevent further oxidation of molten products during the experiments. The whole crucible was either water quenched, or the sampling was carried out by dipping a copper rod onto the surface of the slag. Specimens were studied with LOM, SEM + EDS, and by chemical means.

(2) Melted samples were blown onto the molten slag in an aluminum oxide or a quartz crucible placed in a quartz ampoule (procedure described also in Ref. 23 and Figure

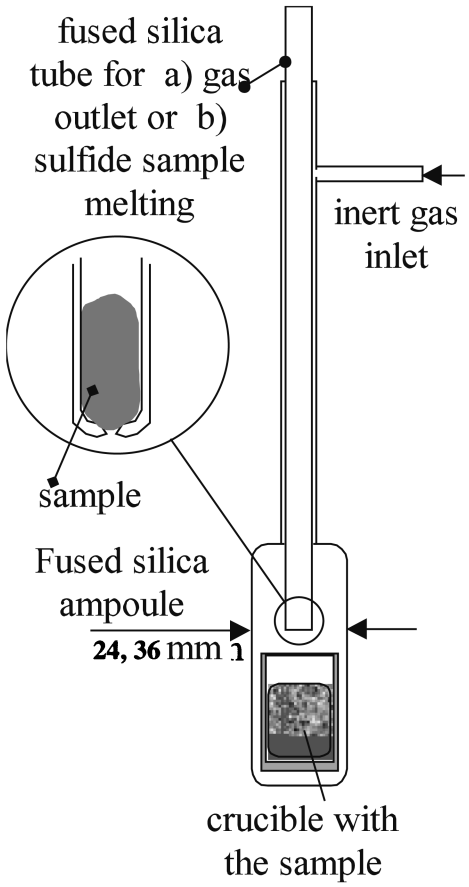

Fig. 5—Simplified schematic presentation of the fused silica ampoule employed in various types of smelting experiments.

Table I. Chemical Analysis of Materials Use

	Chalcopyrite and Matte Samples									Slag Samples		
Wt Pct	CHP Concentrate	OCHP* 1	OCHP* 4	OCHP* 489	OCHP* 10	OCHP* 12	HOC	SHM	MGIM	Wt Pct	V	VI
Cu	23.10	24.6	24.4	24.0	25.3	26.5	35.2	71.3	62.8	Fe	53.5	48.0
Fe	29.50	32.8	32.2	32.0	32.2	30.3	35.0	4.2	16.8	Fe^{2+}	50.6	36.2
S	31.50	30.5	25.4	27.0	22.3	24.9	12.1	24.4	16.7	Fe^{3+}	2.9	11.8
Zn	1.58	—	—	—	—	—	—	—	—	Al_2O_3	—	3.6
Ni	0.15	—	—	—	—	—	—	—	—	FeO	65.1	48.6
Co	0.16	—	—	—	—	—	—	—	—	Fe_2O_3	4.2	16.9
SiO2	7.40	—	—	—	—	—	—	—	—	SiO_2	30.8	32.9
MgO	1.69	—	—	—	—	—	—	—	—	—	—	—
CaO	0.34	—	—	—	—	—	—	—	—	—	—	—
C	0.89	—	—	—	—	—	—	—	—	—	—	—
Σ	96.31	—	—	—	—	—	82.3	99.9	96.3	—	—	—
De-S*	—	0.11	0.25	0.18	0.35	0.27	—	—	—	—	—	—

*Average values, calculated from Cu and Fe balance.

5). The crucible system was heated in the furnace until the slag was molten. Matte powder was charged in a quartz tube, which had a small orifice in the bottom (~1 mm, Figure 5), and melted above the slag before being blown into the molten mixture. The idea was that the surface tension would keep the molten matte in the tube until, with the aid of a rubber bulb pump or pressurized gas, the sample was introduced onto the surface of the slag. The whole ampoule was lifted from the furnace, quenched in water, and polished samples were studied using LOM, and SEM + EDS methods.

(3) The crucible with the reactants, inside the quartz ampoule, was placed in a furnace provided with an X-ray transmission image system, described in recent publications.[26–27] The furnace was heated up to 1350 °C by six $LaCrO_3$ elements at a relatively low heating rate of about 35 °C per hour. The crucible holding the slag sample was brought down to the final temperature zone, and the molten matte sample was introduced to the melt from the upper side of the furnace using the same principle as in technique 2. The position of the ampoule was confirmed by X-ray photography, using continuous radiation at maximum voltage 110 kV and tube current 60 mV. The slag and matte were left to melt for 45 to 60 minutes, and the molten matte was then blown into the slag using a pressure impulse. The sample behavior was followed continuously, and, for more accurate recording of reactions, the generator had to be used in the pulse mode with a voltage of 80 to 85 kV and a current range of 125 to 160 mA, the exposure time being 1.6 seconds. The image received was captured by a DT-2801 image grabber, and image processing was performed with IPPLUS and photomagic software for contrast improvements. When the reaction approached its equilibrium state and the rate slowed down, the ampoule was removed from the furnace and water quenched. Finally, cross sections of the polished specimens were studied and analyzed using LOM and SEM with an energy dispersive spectrometer (EDS).

More than 130 laboratory-scale experiments were carried out, and representative micrographs were chosen for this article. The choice of micrographs depends naturally on the objectivity of the authors, and in some cases it might be appropriate to doubt the observations. It must be noted, however, that the discussion and results are analyzed keeping these limitations in mind and also taking into account previous work of several authors in this area.

D. *Analyses*

Chemical analyses were carried out at Outokumpu Research Oy (Pori, Finland). Oxygen could not be reliably analyzed from heterogeneous sulfide samples, and the determination of magnetite content by saturation magnetization, Satmagan analyzer, also proved to be unreliable due to the presence of sulfide minerals with high magnetic susceptibility (pyrrhotite). The ferric iron content of slag samples was chemically determined, and other analyses were carried out using LOM and a JEOL* JXA 840A SEM equipped with an EDS Tracor Voyager II.

*JEOL is a trademark of Japan Electron Optics Ltd., Tokyo.

Table II. Mixtures Used in the Experiments Matte Separation in Slag

Mixture	OCHP-10 *OCHP-4	MGIM (Pct)	SHM (Pct)	Slag VI (Pct)	Sand (Pct)
1	44	—	—	44	12
2	—	44	—	44	12
3	—	—	44	44	12
4	*40	—	—	40	20
5	—	40	—	40	20
6	—	—	40	40	20

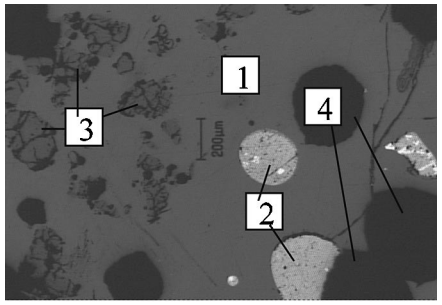

7 min
(*a*)

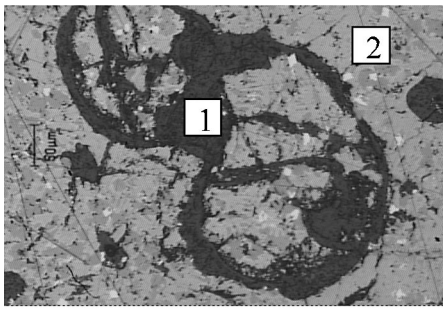

60 min
(*b*)

Fig. 6—LOM micrographs of the quenched sample morphology from mixture 1 obtained after reaction stage (*a*) 7 min and (*b*) 60 min at around 132 °C, showing (1) slag-silica, (2) matte, (3) silica sand, and (4) gas bubbles. Length of scale bar, 200 and 50 μm.

IV. RESULTS AND DISCUSSION

A. *Matte Separation in Slag*

Matte separation in various mixtures of oxidized chalcopyrite, iron silicate slag, and silica sand was investigated at around 1325 °C using experimental method 1 for studying the morphology of quenched samples and observing the change of superficial copper content in the slag. The aim of the experiment was to find out about the magnitude of the separation rate for different mixtures used. Both silica additions were calculated to bring the slag close to (12 pct silica sand) and above (20 pct silica sand) the silica saturation. The composition of the mixtures is shown in Table II, the morphology of quenched samples are in Figures 6 and 7, and results from the sampling tests are summarized in Figure 8.

The reaction and separation morphology of polished samples, shown in Figures 6 and 7, emphasizes the difference

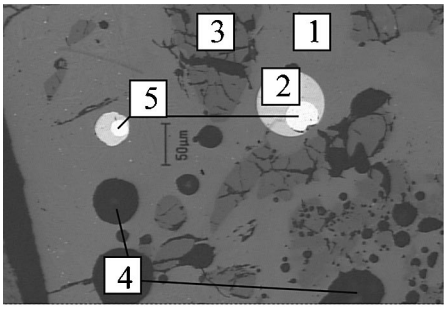

5 min
(*a*)

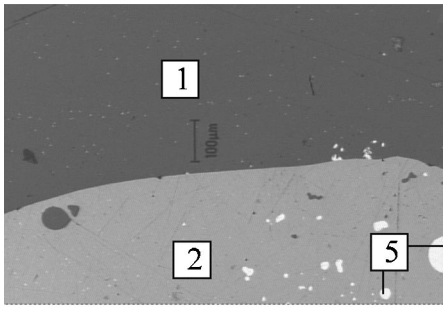

60 min
(*b*)

Fig. 7—LOM micrographs of the quenched samples morphology from mixture 3 obtained after reaction stage (*a*) 5 min and (*b*) 60 min at around 1325 °C, showing (1) slag, (2) matte, (3) silica sand, (4) gas bubbles, and (5) Cu. Length of scale bar, 50 and 100 μm.

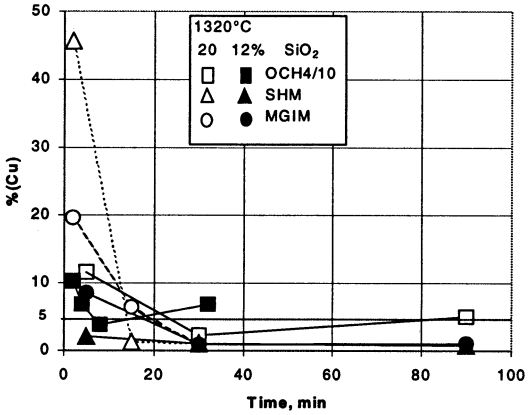

Fig. 8—Superficial copper content of slag as a function of settling time in various mixtures of oxidized chalcopyrite/matte + slag + silica at around 1325 °C.

observed between low- and high-grade matte settling, where the bottom lower-grade matte, in Figure 6(b), showed a consistently high amount of unseparated silica-slag mixture in the structure.

The increase in silica content (20 pct sand) above the saturation limit decreased the matte settling rate in the slag with all the mixtures. Curves in Figure 8 show the sharp settling region, within the first 15 minutes, where most of the matte and slag has separated into two distinctive phases, and after 30 minutes, separation ceases leaving the final copper content of slag. It is suggested that the OCHP settling rate in slag could be somewhat slower than that for higher-grade matte because the same percentage of low- and high-grade matte in slag dictates a higher amount of low-grade droplets. However, with so few experimental points, this behavior cannot fully be confirmed. The sampling method was found to be hard to control, and large quantities of slag were occasionally removed from the crucible. Accordingly, clearly erroneous samples have been removed from Figure 8. It should also be noticed that the MGIM, as industrial matte, is already melted with slag, so OCHP and SHM should, in principle, react more vigorously with slag than MGIM. This behavior was confirmed in morphological studies in Figures 6 and 7, where gas bubbles were observed in the slag, indicating gas evolution by desulfurization reactions, especially with low-grade matte from oxidized chalcopyrite smelting tests (mixtures 1 and 4).

Table III. Mixtures Used in the Experiments Silica Sand Reactions with Matte

Mixture	OCHP-4/g	SHM/g	HOC/g	Silica Sand/g
1	3	—	—	2
2	—	5	—	2
3	—	—	4	0.6

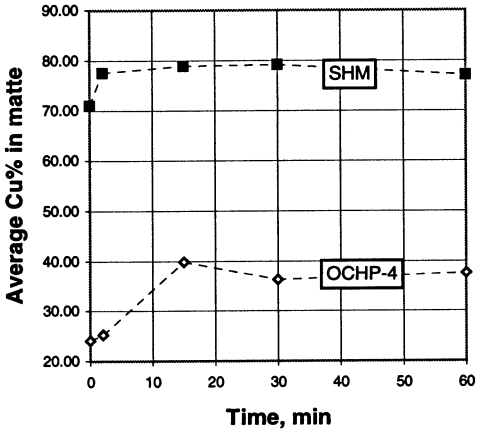

Fig. 9—Average copper content of matte droplets in oxidized chalcopyrite/matte-silica mixtures at around 1300 °C.

B. *Interaction between Oxidized Concentrates and Silica*

The reactions of oxidized chalcopyrite (OCHP-4, HOC) and magnetite saturated high-grade matte (SHM) with silica sand were studied by carefully melting mixed powders at around 1300 °C in an alumina crucible placed in a fused silica ampoule (Figure 5). After a defined period of time, the whole system was lifted from the furnace and quenched in water. Samples were prepared and studied under LOM and SEM, and the average copper content of matte droplets were analyzed using EDS for OCHP-4 and SHM mixtures. Iron content would have been a more reliable indicator for the progress of interaction reactions, but unfortunately, the iron analysis proved to be unreliable due to the effect of the high-iron background environment (iron silicate slag). The composition of mixtures is shown in Table III, and the evolution of copper content with time is presented in Figure 9. It appears that Reactions [1] and [2] tend to proceed in the

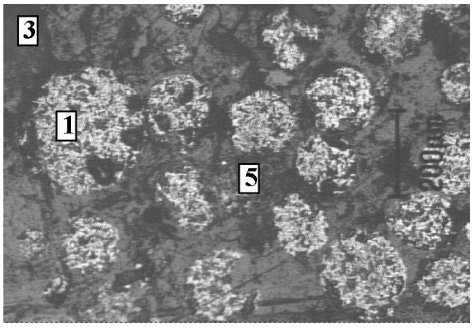

(*a*)

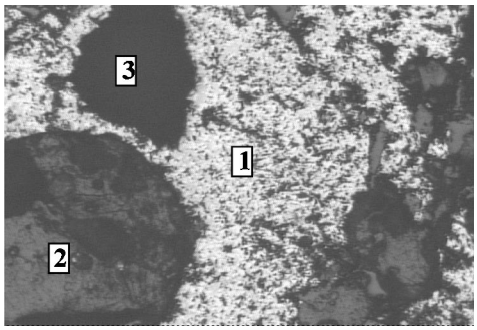

(*b*)

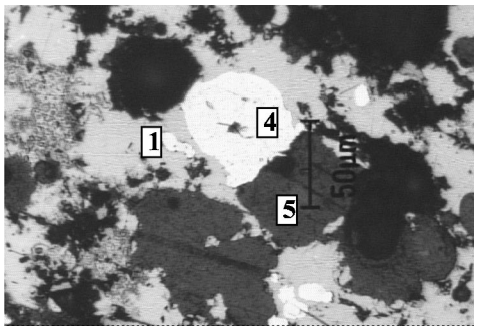

(*c*)

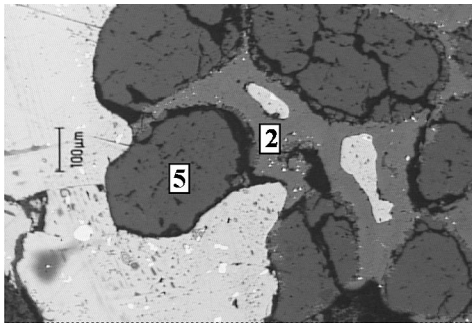

(*d*)

Fig. 10—LOM micrographs of the quenched sample morphology of oxidized chalcopyrite/matte - silica sand mixtures: (*a*) and (*b*) 2 and 60 min around 1325 °C ± 15 °C; and (*c*) and (*d*) 2 and 60 min around 1315 °C ± 15 °C showing (1) matte, (2) slag, (3) gas, (4) metallic copper, and (5) silica sand; length of scale bar, 200 μm, magnification 50 times 50 μm, and 100 μm.

slag. In both analyzed mixtures, the increase in copper content of the matte droplets and, accordingly, slag formation with oxidized sulfide-silica reaction, ceased within 15 minutes. In Figure 10, polished cross sections are shown, displaying the separation and formation of matte and slag phases found with a reaction time of 2 to 60 minutes. Unreacted silica sand in the slag can be seen in Figures 10(a), (c), and (d), and some dissolved or unseparated sand particles were still observed in the matte structure after 60 minutes reaction time.

Table IV. Experimental Conditions and Analyzed Copper Content

Slag (g)	Matte (g)	Cu_2O Added in Slag, %	Time, Min	Pct Cu in Droplets in Slag	Pct Cu in Bottom Matte
6.5	1.5	0	10	—	65.02
6	2	0	60	66.01	61.80
6.8	2.6	0	120	62.08	66.88
5.5	2	25	15	86.84	72.78
6	2.6	25	125	78.89	68.61
5.4	2.3	50	125	87.94	73.72
6.6	2.4	50		unsuccessful	
6.1	2.2	75	10	95.50	78.73
7.1	2.6	75	120	84.98	97.28

C. *Interaction between Matte and Highly Oxidizing Slag*

Although the conditions in these experiments correspond primarily to the converting process, where high-grade matte is converted to blister copper in a highly oxidizing environment, they also have some bearing on bath and suspension smelting processes in general. In the experiments, the mechanism of interaction was studied by placing highly oxidized slag powder V with various amounts of Cu_2O added (Section III–B) on top of the matte powder SHM. Melting was carried out in an alumina crucible placed in a fused silica ampoule at 1345 °C ± 15 °C for 2 hours, quenched in water, and prepared for microscopic examinations. The copper level of the settled matte and inclusions in the slag were estimated by means of an EDS. Experimental conditions and analyzed copper content are shown in Table IV.

Vigorous gas evolution by desulfurization reactions was regularly observed at the beginning of all experiments. The morphology of the samples can be seen in the microstructures shown in Figures 11 through 13. A matte layer between the slag and metallic copper separated with gas gaps was regularly observed in the quenched samples. The gap observed in polished sections in Figure 11 may indicate the existence of a stagnant gas layer between the molten phases but might just as well be caused by gas evolution from the matte during solidification or by more extensive shrinking of the matte in solidification and cooling compared to slag. In Figure 14, the average copper content of the bottom matte and matte-metal droplets in the slag has been presented as a function of the cuprous oxide content addition in slag. The size of the copper/matte droplets in the slag was quite small, and, therefore, the analyses must be studied with caution. The average matte grade in slag, with increasing oxidation level (Cu_2O) of slag, was generally higher than that of settled matte, as illustrated in Figure 14, except for iron silicate slag without cuprous oxide. The matte droplets in slag with a regularly observed copper core, shown in Figure 13, were composed of cuprous sulfide with a low iron content. The bottom matte layer, between the copper and slag phases,

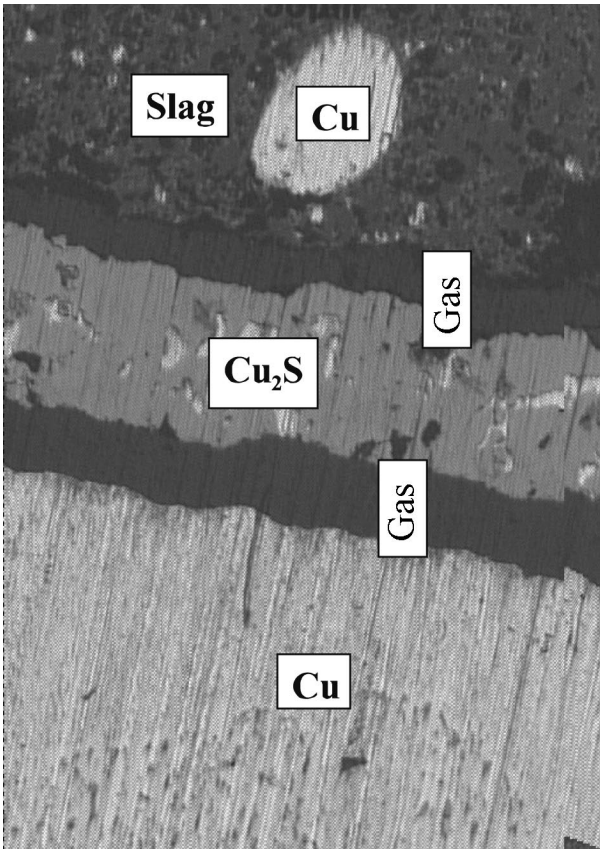

Fig. 11—LOM micrograph of the quenched melting product sample after 125 min reaction time with 50 pct Cu_2O addition in the slag at 1345 °C ± 15 °C. Magnification 20 times.

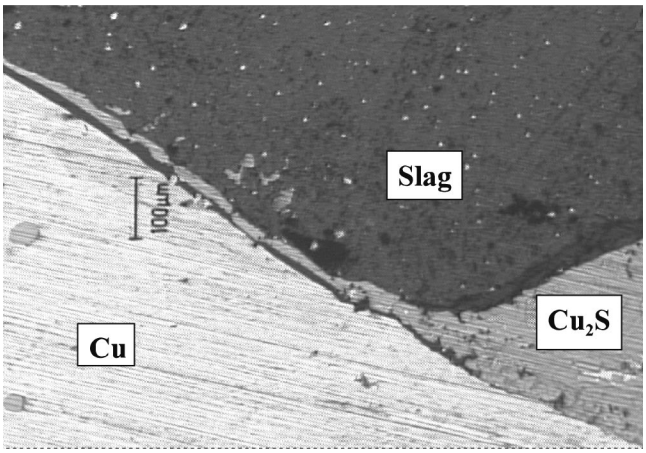

Fig. 12—LOM micrograph of the quenched melting product sample from the bottom part of the crucible obtained after 125 min reaction time with 50 pct Cu_2O addition in slag at 1345 °C ± 15 °C. Length of scale bar, 100 μm.

contained an appreciable amount of iron sulfide even after long exposure times with highly oxidizing slag well capable of oxidizing the iron sulfide present in the matte. This suggests that, in spite of a high driving force, the matte oxidation rate is low, possibly due to the presence of a stagnant gas layer between the molten phases. Furthermore, a common feature in Figure 14 seems to be the decreasing copper matte grade in matte droplets in the slag as a function of settling

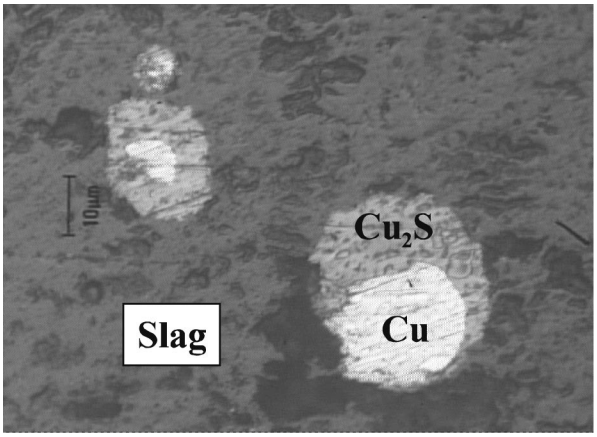

Fig. 13—Typical microstructure of matte droplets (SHM) in oxidized iron silicate slag (10 pct Cu_2O) obtained at 1300 °C, after 15 min settling time. Length of scale bar, 10 μm.

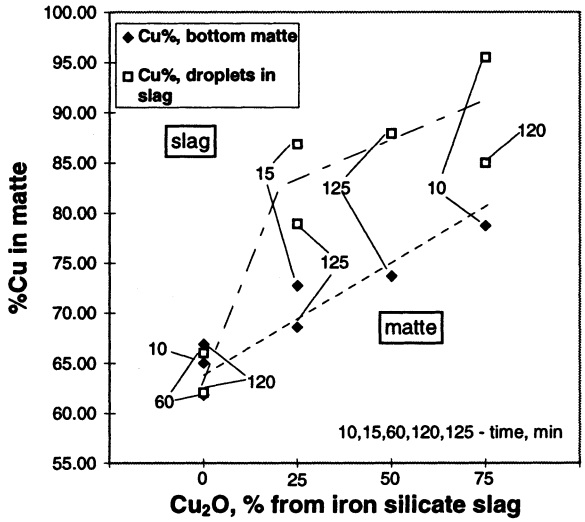

Fig. 14—Copper content of matte settled to the bottom of the crucible *vs* average copper content of matte-copper droplets in slag.

time. However, one has to keep in mind that the amount and size of droplets in the slag decreases continuously with exposure time. Consequently, the accuracy of the analysis also decreases, thus, and no firm conclusions based on the results in Figure 14 can be drawn.

D. *Interaction of Molten Sulfides with Iron Silicate Slag*

The reaction, flotation, and settling phenomena of copper matte-slag was investigated using two methods: technique (2), where melted, quenched, and polished samples were studied using SEM + EDS; and technique (3), X-ray transmission for continuous observation of phenomena occurring during interaction. The resolution in X-ray transmission experiments was found to be poor with fayalite type slags, therefore, low iron wollastonite slags (15 and 22 pct CaO) were employed. In the series using the quenching technique, the sulfide materials were OCHP-1, OCHP-10, and SHM, and in X-ray experiments the sulfide materials consisted of OCHP-10 and SHM.

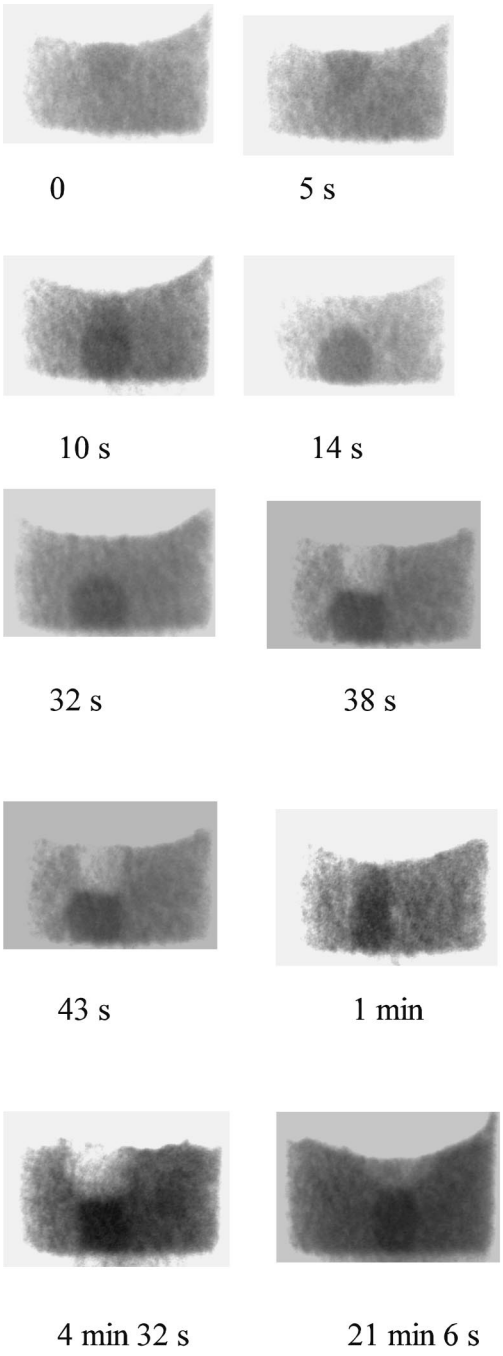

Fig. 15—X-ray image sequence of SHM droplet behavior in wollastonite slag at 1350 °C showing settling, gas formation, and breaking up.

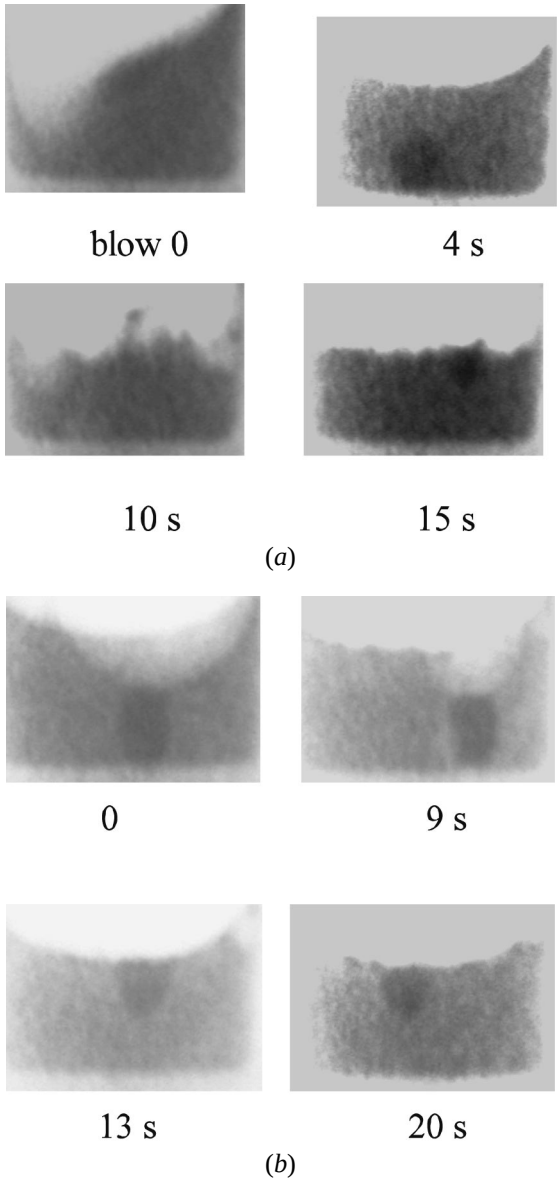

Fig. 16—X-ray images of flotation phenomena due to reactions, gas formation of (*a*) OCHP-10 and (*b*) SHM droplets, at 1350 °C, in wollastonite slag.

According to the X-ray observations, oxidized chalcopyrite (OCHP-10) and magnetite SHM showed intensive interaction with slag and vigorous evolution of gas during the first 10 to 20 minutes period of time. Molten sulfide droplets were bursting and breaking up due to reactions on the droplet surface, as shown in Figure 15. Furthermore, droplets were flotated to the slag surface by evolving gas (Figure 16), where they coalesced and settled back to the bottom if they were of sufficiently large size, as in Figure 17. However, some droplets were retained on the surface by surface forces, and it was experimentally observed that the maximum size of these floating droplets was about 0.5 cm in diameter, shown in Figure 18. Vanyukov and Zaitsev,[28] who carried out X-ray transmission studies on the matte-slag separation and formation, observed the same phenomena and reported a maximum size of floating copper matte droplets of 3 to 5 mm in diameter.

The critical radius of a sphere (R) that can rest at the interface can be calculated using the equation by Maru *et al.*[29]

$$R = 1.27 \left(\frac{\Delta\rho_{23} \cdot g(\Delta\rho_{12} - \Delta\rho_{23})}{\gamma_{23} \cdot \Delta\rho_{23}} \right)^{(1/2)} \quad [8]$$

and Poggi *et al.*[30]

$$R = \left(\frac{2 \cdot \gamma_3}{4/3 \cdot \rho_1 \cdot g} \right)^{1/2} \quad [9]$$

where R is the critical radius of sphere (cm), $\Delta\rho$ is the absolute difference between the densities of the two phases (g/cm^3), g is the gravity constant (m/s^2), γ is the surface

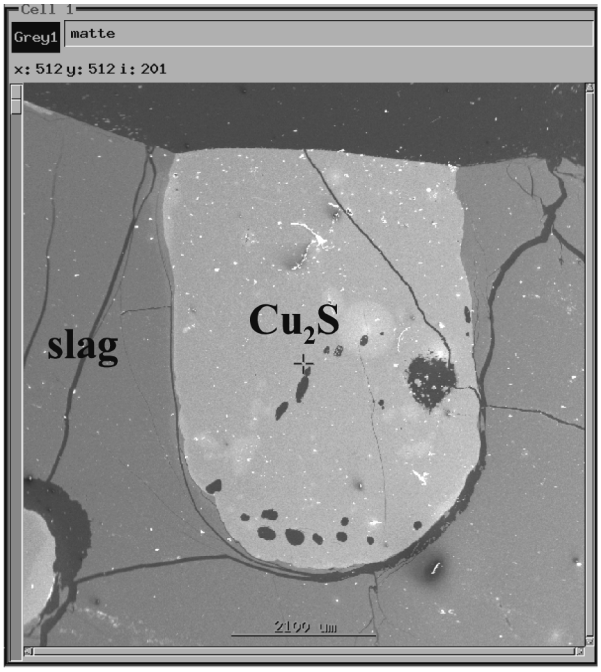

(*a*)

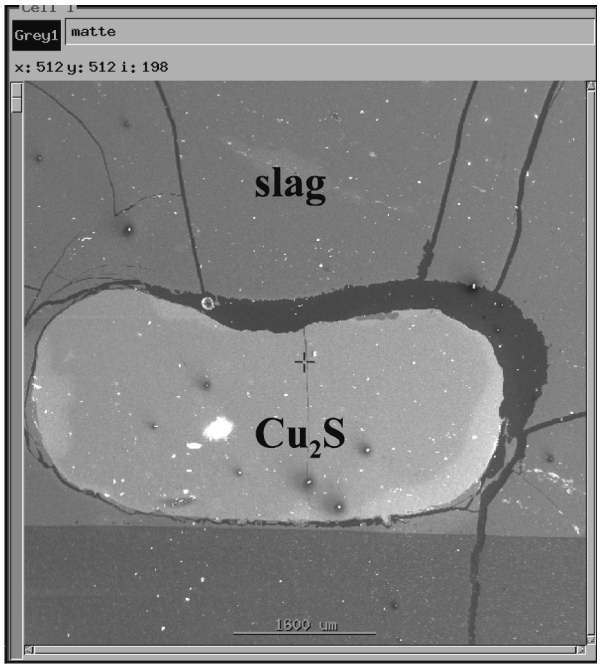

(*b*)

Fig. 17—SEM images of high grade matte (SHM) droplets from (*a*) the surface and (*b*) the lower part of the crucible, at 1350 °C, and wollastonite slag. Length of scale bar, 2100 and 1600 μm.

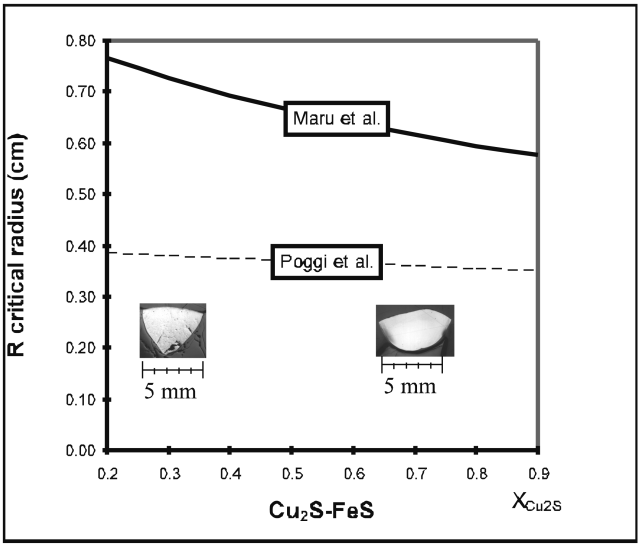

Fig. 18—Theoretically calculated critical radius of a sphere that can rest at the surface of the matte/slag interface in comparison with typical experimentally observed shapes and sizes of droplets. LOM images of matte droplets on top of the slag surface from the quenched samples in X-ray experiments at 1350 °C.

tension (mN/m), and subscripts 1 particle/drop, 2 exit phase (gas), 3 entry phase (slag).

In Eq. [9], the theoretical maximum size floating drop is obtained by equating the upward force due to surface tension $2\pi r_D \gamma_S$ and weight $4/3\pi r_D^3 \rho_D g$. Smaller droplets will float, while larger drops would be expected to sink through the surface.[30] The density of slag and matte and the experimental surface and interfacial tension values used in Eqs. [8] and [9] (shown in Figure 18) were taken from the literature.[31,32,33] In the equation by Maru *et al.*,[29] it is assumed that the contact angle is 180 deg, and according to Rapacchietta *et al.*,[34] the critical size of particles floated on the interface increases with increasing contact angle. It should be noted that the experimentally observed metallic drops in this study are not spherical, and these equations do not strictly apply. However, Utigard *et al.*[35] propose that the calculation procedure in Eq. [8] seems to describe the flotation behavior reasonably well, at least in liquid metal-sodium flux systems.

Ip and Toguri[36] found, in their surface and interfacial tension measurements, that matte flotation in the slag phase by rising gas bubbles cannot be eliminated by altering the matte grade or composition, while it can be avoided by maintaining the oxygen pressure below 10^{-9} bar. The results in this study confirm the flotation of low-grade and high-grade matte. If, on the other hand, the radius of floating droplets increases beyond the critical size, they will settle through the slag phase. A higher rate of coalescence and a bigger droplet size would, therefore, also prevent the floating of dispersed droplets by rising gas bubbles. On the basis of the results discussed, the increasing matte grade might increase the matte droplet size and decrease the amount of stabile floating droplets. According to Vanyukov and Zaitsev,[28] the flotation of matte droplets will increase the coagulation of droplets rather than lead to emulsification of the matte.

Finely dispersed matte in slag was observed in the quenched samples of slightly oxidized (OCHP-1) and moderately oxidized (OCHP-10) chalcopyrite experiments (Figures 19 and 20). It cannot be confirmed for sure whether the dispersion is due to the breaking up of droplets by vigorous reactions or the precipitation of dissolved matte during solidification of slag. Gas evolution by matte-slag reactions was also revealed by the presence of gas bubbles and/or a gap between phases in the quenched samples (not shown in

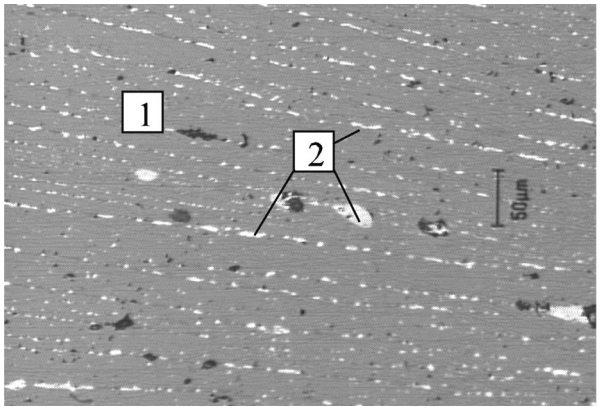

(*a*)

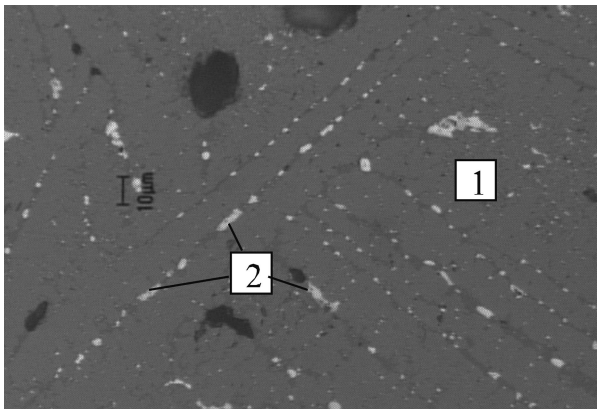

(*b*)

Fig. 19—Typical microstructures obtained with (*a*) OCHP-1, 5 min settling time, and (*b*) OCHP-10, 30 min settling time, in iron silicate slag at 1300 °C showing (1) slag and (2) matte in slag. Length of scale bar, 50 and 10 μm.

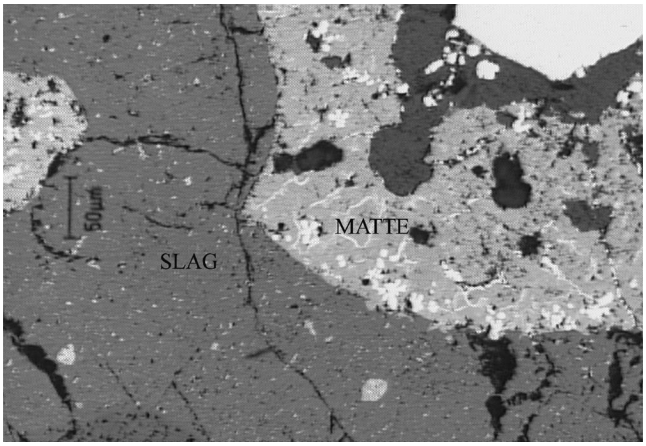

Fig. 20—LOM micrograph of OCHP-10 in iron silicate slag from the bottom of the crucible at 1300 °C. Length of scale bar, 50 μm.

micrographs). High-grade matte droplets were generally spherical (Figure 21) in contrast to the low-grade matte shown in Figure 19. Both quenching and X-ray tests suggest a higher settling and separation rate of high-grade matte (> 70 pct Cu) compared to that of low-grade matte (35 to 45 pct Cu).

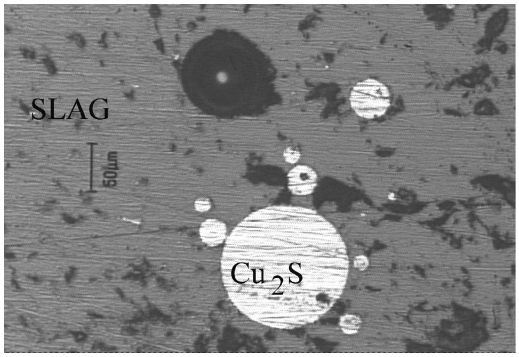

Fig. 21—Typical microstructures obtained with SHM droplets in iron silicate slag obtained at ~1340 °C with 120 min settling time. Length of scale bar, 50 μm.

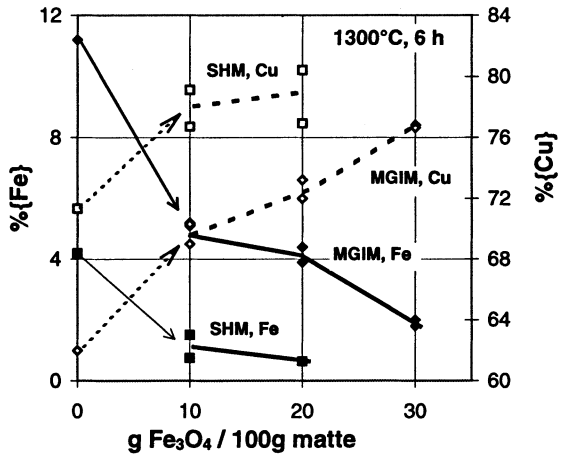

Fig. 22—Change in matte composition as a function of magnetite addition, with constant amount of silica, in matte-magnetite-silica mixture.

E. *Slag Formation in Matte Environment and Residual Silica*

Microscopic examinations of reaction and separation experiments revealed a relatively high silica content and a large amount of inclusions in the matte phase. Silica removal from the matte through the slag forming Reaction [1] was studied by melting powdered mixtures of industrial (MGIM) and synthetic high-grade matte (SHM), magnetite and silica sand, holding at 1300 °C for 6 hours in silica crucibles, and then cooling rapidly in water. The added silica sand content in the mixture was 30 g per 100 g of matte, and the magnetite content varied from 10 to 30 g per 100 g of matte. The chemically analyzed average residual silica content in matte, and the average matte composition (copper and iron), are presented in Figures 22 and 23. High silica inclusions, demonstrated in Figure 24, were mainly composed of iron and silica (oxides). Slag formation, a thin slag circle, on the outer surface of the sample attached to the crucible wall was observed.

By comparing the results from this research with Yazawa's and Jalkanen's findings,[37–40] the reliability of the solubility data can be evaluated, as shown in Figure 25. From the solubility data of Yazawa, it can be seen that the SiO_2 in the matte of $30Cu_2S$ and 30FeS was little more than 1 pct,

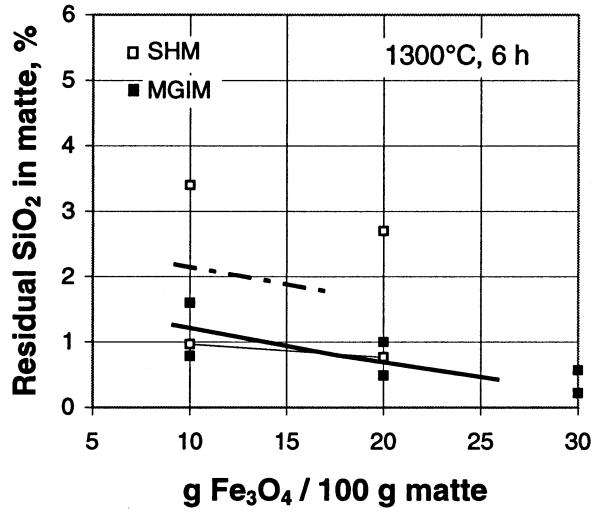

Fig. 23—Residual silica content of matte as a function of magnetite addition in the matte-magnetite-silica mixture.

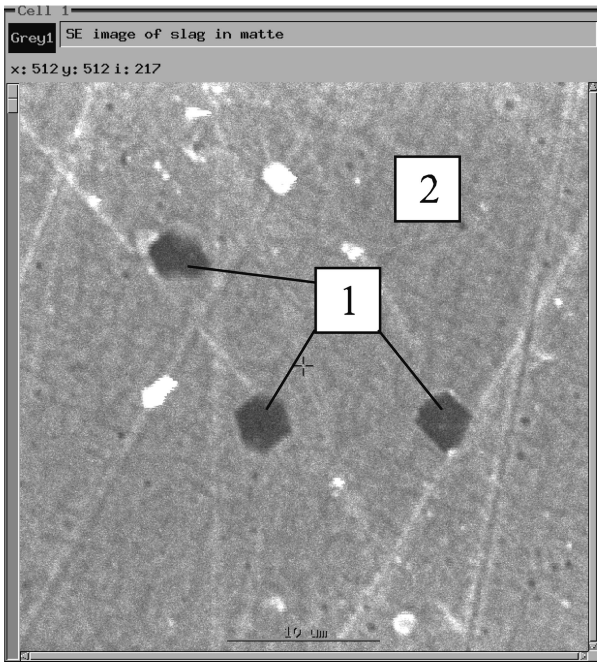

Fig. 24—SEM micrograph of MGIM, magnetite and silica mixture, showing (1) silica inclusions in matte and (2) matte, obtained at 1300 °C, 6 h settling time. Length of scale bar, 10 μm.

being at maximum matte grade in Yazawa's study, 38 pct Cu, about 1.3 pct. The general trend of decreasing silica content in the matte with increasing matte grade was also observed in this study. However, SEM micrographs indicated that the high silica contents analyzed in the matte after 6 hours settling time resulted in insufficient settling of both primary silica sand and iron silicate particles, as well as a very small particle size precipitate of silica dissolved in the molten matte. The results of this study cannot be directly compared with those of Yazawa and Jalkanen. It is quite obvious that the analyzed high silica values are due to insufficient separation of the silica or iron silicate phase, formed as a result of Reaction [1].

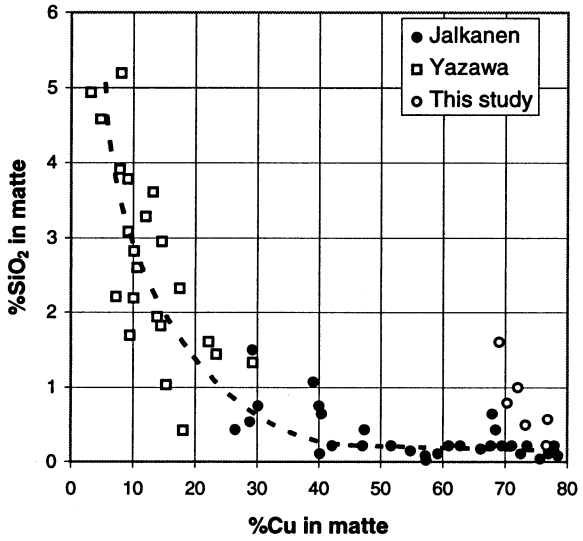

Fig. 25—Silica content of matte as a function of matte grade (data taken from Refs. 37 through 40).

V. CONCLUSIONS

There are certain limitations to the conclusions that can be drawn from experimental observations in this study relating to industrial processes. (1) A lack of unambiguous data from pilot or production scale furnaces caused problems in planning proper experiments. (2) It is not a straightforward task to draw conclusions from microscale experiments of matte and slag formation and separation phenomena relating to industrial smelting units. (3) The investigation conducted in this study is more phenomenological in character and is largely based on visual observations that are open to subjective misinterpretations.

Keeping these limitations in mind, the following conclusions were drawn:

1. The results of this investigation support the idea that desulfurization and deironization of matte, as well as slag formation, are completed in the settler region as a result of magnetite/ferrite interaction with iron sulfides in the matte.
2. The production of sulfur dioxide gas inside the molten bath is possible up to a certain iron sulfide content in the matte. The breaking up of reacting matte droplets by vigorous gas evolution might also be possible, thus enhancing the emulsification of matte in the slag.
3. Matte droplet flotation by sulfur dioxide formed at the matte-slag interface occurs independently of the copper content in the matte. Under the conditions prevailing in the industrial furnace, flotation phenomena will enhance the coagulation and settling rate of matte droplets through the slag rather than accelerate the emulsification of matte droplets.
4. Silica sand particles, enclosed inside high-grade matte, tend to react slowly with iron oxides available in the matte. The separation rate of silica containing inclusions in the matte seemed to be low (6 hours was not enough to reach equilibrium solubility level). This can lead to a higher silica content in the industrial matte than the chemical solubility suggests.
5. Based on experiments with oxidizing slag, it is suggested

that large high-grade matte droplets will not necessarily have enough time to reach the oxidation degree of slag, even when passing through highly oxidizing slag. This could lead to differences in the average oxidation degree of slag and matte in the settler.

ACKNOWLEDGMENTS

Financial support for this work was provided by the Finnish Cultural Foundation, the Walter Alhström Foundation, the Foundation for Research of Natural Resources in Finland, and the Outokumpu Foundation. Outokumpu Research Oy (Pori, Finland) provided chemical analyses for this study. We thank P. Nurmi and L. Palmu for their assistance in carrying out experiments.

REFERENCES

1. F.R.A. Jorgensen and E.R. Segnit: *Proc. Aus. Inst. Min. Metall.*, 1977, pp. 39-46.
2. F.R.A. Jorgensen: *Proc. Aus. Inst. Min. Metall.*, 1983, pp. 37-46.
3. F.R.A. Jorgensen, F.J. Moyle, and M.W. Wadsley: *Flash Reaction Processes, Int. Conf.*, D.G.G. Robertson, H.Y. Sohn, and N.J. Themelis, eds, University of Missouri–Rolla, Rolla, MO, 1988, pp. 167-90.
4. A.T. Jokilaakso: *Acta Polytechn. Scand.*, 1992, ch. 205.
5. A.T. Jokilaakso, R.O. Suominen, P.A. Taskinen, and K.R. Lilius: *Trans. Inst. Min. Metall. C*, 1991, vol. 100, pp. C79-C90.
6. H.Y. Sohn and P.C. Chaubal: *Metall. Trans. B*, 1993, vol. 24B, pp. 975-85.
7. A. Otero, J.K. Brimacombe, and G.G. Richards: *Pyrometallurgy of Copper*, C. Diaz, C. Landolt, A. Luraschi, and C.J. Newman, eds., Pergamon Press, New York, NY, 1991, pp. 459-73.
8. G.J. Morgan and J.K. Brimacombe: *Metall. Mater. Trans. B*, 1996, vol. 27B, pp. 163-75.
9. R.D. Hagni and C.B. Vierrether: *Flash Reaction Processes, Int. Conf.*, D.G.G. Robertson, H.Y. Sohn, and N.J. Themelis, eds., University of Missouri–Rolla, Rolla, MO, 1988, pp. 245-69.
10. R.D. Hagni, C.B. Vierrether, and H.Y. Sohn: *Metall. Trans. B*, 1988, vol. 19B, pp. 719-29.
11. T. Kimura, Y. Ojima, Y. Mori, and Y. Ishii: *The Reinhardt Schumann Int. Symp. on Innovative Technology and Reactor Design in Extraction Metallurgy*, D.R. Gaskell, J.P. Hager, J.E. Hoffmann, and P.J. Mackey, eds., TMS-AIME, Warrendale, PA, 1986, pp. 403-18.
12. E.H. Partelpoeg: *Flash Reaction Processes, Int. Conf.*, D.G.G. Robertson, H.Y. Sohn, and N.J. Themelis, eds., University of Missouri–Rolla, Rolla, MO, 1988, pp. 35-45.
13. N. Kemori, Y. Ojima, and Y. Kondo: *Flash Reaction Processes, Int. Conf.*, D.G.G. Robertson, H.Y. Sohn, and N.J. Themelis, eds, University of Missouri–Rolla, Rolla, MO, 1988, pp. 47-67.
14. N. Kemori, W.T. Denholm, and H. Kurokawa: *Metall. Trans. B*, 1989, vol. 20B, pp. 327-36.
15. Y. Kuprjakov: *Metallurgiya*, 1979, pp. 69-76.
16. N.J. Themelis, L. Wu, and Q. Jiao: *Flash Reaction Processes, Int. Conf.*, D.G.G. Robertson, H.Y. Sohn, and N.J. Themelis, eds., University of Missouri–Rolla, Rolla, MO, 1988, pp. 263-85.
17. K. Genevski, P. Bakarjiev, and M. Mantsevich: *Conf. on the Occasion of 230th Anniversary of Founding the Mining Academy in Banska Stiavnica*, Kosice, 1992.
18. N. Kemori, Y. Shibata, and K. Fukushima: *JOM*, 1985, pp. 25-29.
19. Y.H. Kim and N.J. Themelis: *Int. Symp. on Innovative Technology and Reactor Design in Extraction Metallurgy*, D.R. Gaskell, J.P. Hager, J.E. Hoffmann, and P.J. Mackey, eds., TMS-AIME, Warrendale, PA, 1986, pp. 349-69.
20. H. Jalkanen and O. Mäenpää: Report, Outokumpu Oy, Pori, Finland, 1970.
21. D.L. Kaiser and J.F. Elliot: *Metall. Trans. B*, 1988, vol. 19B, pp. 935-41.
22. F. Johanssen and H. Knahl: *Erzmetallurgy*, 1963, vol. 12, pp. 611-74.
23. K. Fagerlund, H. Jalkanen, P. Nurmi, and P. Taskinen: *EPD Congr.*, B. Mishra, ed., TMS-AIME, Warrendale, PA, 1997, pp. 635-47.
24. K. Fagerlund, L. Palmu, and H. Jalkanen: *Sulfide Smelting '98 Current and Future Practices*, J.A. Asteljoki, and R.L. Stephens, eds., TMS-AIME, Warrendale, PA, 1998, pp. 375-85.
25. K. Fagerlund: *Acta Polytechn. Scand.*, Ph.D. Thesis, Helsinki University of Technology, Helsinki, 1998, ch. 258.
26. X. Shuang and L.E.K. Holappa: *Steel Res.*, 1994, vol. 65, pp. 511-16.
27. M. Liukkonen, L.E.K. Holappa, and D. Mu: *5th Int. Conf. on Molten Slags, Fluxes and Salts '97*, ISS, Sydney, 1997, pp. 163-68.
28. A.V. Vanyukov and V.Y. Zaitsev: *Metallurgiya*, (Leningrad) In Russian; Russian summaries, 1969, pp. 235-69.
29. H.C. Maru, D.T. Wasan, and R.C. Kintner: *Chem. Eng. Sci.*, 1971, vol. 26, pp. 1615-28.
30. D. Poggi, R. Minto, and W.G. Davenport: *J. Met.*, 1969, Nov., pp. 40-45.
31. T. Nakamura and J.M. Toguri: in *Pyrometallurgy of Copper*, C. Diaz, C. Landolt, A. Luraschi, and C.J. Newman, eds., Pergamon Press, New York, NY, 1991, pp. 537-51.
32. M. Kucharski, S.W. Ip, and J.M. Toguri: *Can. Metall. Q.*, 1994, vol. 33, pp. 197-203.
33. *Slag Atlas*, 2nd ed., Verlag Stahleisen GmbH, Dusseldorf, 1995.
34. A.V. Rapachietta, A.W. Neumann, and S.N. Omenyi: *J. Colloid Interface Sci.*, 1977, vol. 59, pp. 555-67.
35. T. Utigard, J.M. Toguri, and T. Nakamura: *Metall. Trans. B*, 1986, vol. 17B, pp. 339-46.
36. S.W. Ip and J.M. Toguri: *Metall. Trans. B*, 1992, vol. 23B, pp. 303-11.
37. H. Jalkanen: *Scand. J. Met.*, 1981, vol. 10 pp. 177-84.
38. H. Jalkanen, L. Holappa, and J. Mäkinen: *Advances in Sulfide Smelting*, H.Y. Sohn, D.B. Geirge, and A.D. Zunkel, eds., TMS-AIME, Warrendale, PA, 1983, vol. 1, pp. 277-92.
39. H. Jalkanen and M.H. Tikkanen: *Scand. J. Met.*, 1979, vol. 8, pp. 133-39.
40. A. Yazawa: *Tech. Rep. Tohoku Univ.*, 1956, pp. 31-50.